CHAPTER 3: RESEARCH METHODOLOGY

3.1 Introduction

This chapter describes the materials employed and the procedures undertaken to prepare forsterite bodies. Additionally, the techniques by which the forsterite ceramic were characterized for their density, phase stability and phase composition and mechanical properties are discussed in this chapter. Forsterite (Mg_2SiO_4) is one of the potential bioceramic that is suitable for load bearing application compared to its counterpart, hydroxyapatite (HA) which exhibits excellent biocompatibility properties but it is also known to have poor mechanical characteristics. This chapter describes the hypothesis development and synthesis method used to sinter the forsterite ceramic samples by conventional pressureless sintering with the aim of improving its mechanical properties particularly the fracture toughness.

3.2 Forsterite Powder Synthesis

The creation of pure, dense forsterite ceramic with superior mechanical properties demands a process to prepare the stoichiometric forsterite powder. This follows a typical process of raw materials selection, synthesis of forsterite powder, filtering, washing and drying of synthesized powder. The details of this process are discussed herein. The synthesis of forsterite powder involved mixing the following starting precursors at a weight ratio of 1 to 1.88 based on the stoichiometric equation given in Eqn. 3.1. In a typical experiment, the two starting precursors are magnesium oxide (MgO; 97% purity, Merck) and talc ($Mg_3SiO_4O_{10}(OH)_2$; 99% purity, Sigma Aldrich). The detailed calculation is provided in Appendix A.

$$Mg_3Si_4O_{10}(OH)_2 + 5\ MgO \rightarrow 4\ Mg_2SiO_4 + H_2O \qquad \text{(Eqn. 3.1)}$$

3.2.1 Powder Optimization

Investigation on the powder synthesis parameters including ultrasonic mixing parameters, ball milling time and heat treatment were carried out before finalizing the powder synthesis method. The best ball milling duration and ultrasonification method will be reported in section 3.3. The most efficient heat treatment dwell time will be reported in section 3.5.

3.2.1.1 Effect of Direct Ultrasonification

Ultrasonic vibration with amplitude of 30% and 50% generated by ultrasonic processor (20 kHz, Cole-Parmer, U.S.A.) was applied by immersing directly the probe into the powder mixed with 150 ml of ethanol solvent in a beaker for 2 hours with pulse rate of 1 minute on and 10 seconds off. This cooling interval period of 10 seconds was necessary to prevent overheating during high intensity ultrasonification. The quantity of amplitude was maintained constant by the generator with maximum power output of 500W. The ultrasonification helps to break up agglomerates in the mixture and to promote powder homogenization (Oliveria et al, 2002). Heat treatment at 1200°C for 2 hours was performed followed by X-ray diffraction (XRD) examination to check the phase composition of the mixtures.

3.2.1.2 Effect of Ball Milling after Direct Ultrasonification

The effect of 1 hour and 3 hours ball milling was investigated on the two mixtures applied with 2 hours direct ultrasonification at amplitude of 30% and 50%. In addition, each sample was subjected to 2 hours of heat treatment at 1200°C. Lastly, XRD phase analysis was performed.

3.2.1.3 Effect of Heat Treatment

Direct ultrasonification 50% amplitude with 3 hours ball milling was compared with indirect ultrasonification with 3 hours ball milling. The two starting powders were mixed together in ethanol by subjecting to ultrasonic bath which is also known as indirect ultrasonification at a fix intensity of 28-34 kHz. The two powder components were mixed with 150 ml of ethanol in a beaker which was immersed inside the ultrasonic bath unit filled with water. The total duration of indirect ultrasonification was 22 minutes. Heat treatment at 1200°C and 1250°C for 2 hours were performed to study the phase composition from XRD phases.

Heat treatment of 1 hour at different temperatures (1200°C, 1300°C and 1400°C with ramp rate of 10°C per minute) was performed on the samples earlier subjected to indirect ultrasonification and 3 hours ball milling. The XRD results were compared with previous heat treatment conditions (1200°C and 1250°C for 2 hours with ramp rate of 10°C per minute).

The samples were subjected to heat treatment at 1400°C for 2 hours, 1 hour and 1 minute to study the effect of dwell time on phase composition.

3.3 Ball Milling and Drying

Based on the preliminary study for powder optimization in Section 3.2.1, indirect ultrasonifcation and ball milling duration of 3 hours at 350 rpm were selected for sintering studies. The slurry was transferred into a 500 ml high density polyethylene bottle for ball milling process which will further enhance powder homogenization (Oliveria et al., 2001) by breaking up any agglomerates left from the indirect ultrasonification process. The bottle was filled with 2 mm diameter sized zirconia balls measuring 200 ml and 150 ml ethanol and placed on the cascading milling machine. The slurry was filtered and dried in an oven (Memmert, Germany) at 60°C for 24 hours after the ball milling procedure has completed. Upon completion of drying process, the dried powder was sieved using a 212 µm size mesh stainless steel sieve (Endecotts, England). The sieved powder was stored in a dry box with relative humidity set at 45% until it is required for further experiment.

3.4 Forsterite Green Body Preparation

Two types of forsterite green body (circular disc & rectangular bar) were prepared for the experiment. A stainless steel circular and rectangular bar dies were cleaned with WD-40 lubricant to remove any contaminants. The cleaning procedure was repeated before each pressing to make sure no contaminants were present. Typically about 1.8 g and 2.0 g of forsterite powders were weighed and filled into the circular disc and rectangular bar die, respectively. Compaction pressure of 2.5 to 3.0 MPa was applied for 5 seconds using a uniaxial press machine to form circular disc with 20 mm in diameter by 5 mm thickness and rectangular bar green samples having dimensions of 32 × 13 × 6 mm. Previous study has shown that green samples fabricated by uniaxial pressing are known to lose uniformity and develop cracks upon sintering (Muralithran & Ramesh, 2000) and that nanocrystalline ceramic powders are difficult to compact. The green

samples were subjected to cold isostatic pressing (CIP) at 200 MPa prior sintering. Samples subjected to CIP process are known to experience a uniform shrinkage. Moreover, this would lead to a uniform densification when it is sintered (Ramesh *et al.*, 2004).

3.4.1 Grinding and Polishing

Surfaces of the sintered disc compacts were subjected to grinding and polishing prior to properties determination. A rough silicon carbide (SiC) paper of grade 600 was used for the first round of grinding. The speed of the grinding machine was set to 300 rpm. Constant supply of water acted as the cooling agent throughout the grinding process. At the end of the first round, smoother surface with significant scratch marks were visible. This is followed by second round of grinding using a finer SiC paper (grade 800). The forsterite compact was rotated 90° clockwise and subjected to grinding for another 5 minutes until the perpendicular grinding marks were canceled out creating a smoother surface. Similar procedure was repeated for the final grinding process using a fine SiC paper (grade 1200). At the end of the third round shiny surface was visible. The forsterite compacts must be maintained at similar position with equal force during the grinding process to minimize concave edges and uneven surface.

After the grinding was completed, the fosterite compacts were polished to obtain smooth and shiny surface which is pre-requisite for surface analysis such as micro-hardness test and FESEM analysis. For this purpose, 3 µm and 1 µm diamond paste were used for rough and fine polishing of the forsterite compacts. The 3 µm diamond paste was spread evenly on the polishing cloth and silica based fluid was used as the lubricant. The polishing machine speed was set to 300 rpm. The polishing was carried

out for 10 minutes for each samples and then repeated the same using 1 µm diamond paste to obtain shiny, reflective surface.

3.5 Sintering Profile

Sintering is the process whereby inter particle pores in a granular material are eliminated by atomic diffusion driven by capillary forces during a heat treatment process (Chaim et al., 2008). Physical shrinkage of the samples signifies densification has taken place with the removal of the porosity (Bernard-Granger at al., 2008). In order to determine the shrinkage percentage, the physical dimensions of the forsterite compacts before and after sintering were recorded.

3.5.1 Sintering Profile Optimization

Two set of samples were studied to determine the optimized sintering profile. Sample set no. 1 would subject the forsterite powder to 3 hours ball milling followed by heat treatment at 1400˚C for 1 hour prior to compaction and sintering. Sample set no. 2 would subject the forsterite powder to 3 hours ball milling followed by compaction and sintering without heat treatment.

The samples for both set no.1 and no.2 were sintered at temperatures 1200˚C, 1300˚C, 1400˚C and 1500˚C for 2 hours at a ramp rate of 10˚C per minute. This sintering temperatures are within the typical solid state sintering temperature range which is between 0.6 to 0.9 (De Jonghe & Rahman, 2003) of the forsterite's melting point which is 1890°C (Klein & Hurlbut, 1985). Each sintering profile was subjected to 10°C/min ramp rate (heating and cooling). The sintering process was carried out in an electric furnaces (LT Furnace, Malaysia). The sample set that produce pure phase forsterite with

least secondary phase will be selected as the optimized sintering profile for densification behaviour study. This result will be discussed in Chapter 4.3.

3.6 Characterization of Forsterite Compacts

3.6.1 Bulk Density Measurement

The densi-meter balance (Shimadzu AY220, Japan) was used to measure the bulk densities of the forsterite disc and bar compacts based on the water immersion technique, in accordance to the Archimedes principle. According to this principle, the upward buoyant force that is exerted on a body immersed in a fluid either partially or fully submerged, is equal to the weight of the fluid that the body displaces (Acott, 1999). Applying this principle into the densi-meter, the forsterite disc and bar compacts were inside a beaker filled with distilled water placed onto the balance eventually buoy up by the displaced water. The recorded increment in weight by the balance represented this force. Therefore the density can be calculated using the recorded weight values in air and water using Equation 3.2.

$$\rho = \frac{w_a}{w_a - w_w} \times \rho_w \qquad \text{(Eqn. 3.2)}$$

Where,

ρ = Bulk density of the sample

ρ_w = Density of distilled water

w_a = Weight of sample in the air

w_w =Weight of sample in the water

Using the calculated bulk density, the relative density is calculated using Equation 3.3.

$$\rho_R = \frac{\rho}{\rho_{TH}} \times 100\% \qquad \text{(Eqn. 3.3)}$$

Where,

ρ_R = Relative density, in percentage

ρ = Bulk density of the sample

ρ_{TH} =Theoretical density of forsterite which is taken as 3.221 g/cm^3 (Ghomi et al., 2011)

3.6.2 Vickers Hardness Evaluation

Hardness is one of the most frequent measured properties of ceramic material which help to characterize the resistance to deformation, densification, and fracture. Hardness is usually measured on conventional micro hardness machines having Vickers diamond indenters. These machines make impressions whose diagonal size is measured with an attached optical microscope. In this experiment, indentations were produced using the Vickers micro hardness tester (HMV, Shimadzu, Japan) with a pyramidal diamond indenter having 136° tip angle. In a typical experiment, a load of 200 g is applied smoothly without impact and hold for 10 seconds during the indentation process as per ASTM E384-10 standard (ASTM, 2010a). After removal of the load, the diagonal lengths of the diamond shaped indentation were measured using the optical microscope (Olympus, Japan). Five indentations were produced for each forsterite disc compact and average value taken. The formula used to calculate the Vickers Hardness is given in Equation 3.4.

$$H_v = \frac{1.854 \times P}{(2a)^2} \quad \text{(Eqn. 3.4)}$$

Where,

H_v = Vickers Hardness

P = Applied load

2a= Average diagonal length = $\frac{d_1+d_2}{2}$, where d_1 & d_2 are the diagonal length as shown in Figure 3.1

3.6.3 Fracture Toughness Evaluation

The indentation method has been shown to be useful in characterizing the hardness of ceramic materials and in evaluating the fracture toughness (Anstis et al. 1981; Chantikul et al., 1981; Evans, 1988; Rizkalla & Jones, 2004; Mullins et al., 2007; Quinn, 1998; Kruzic et al., 2009). The advantages of this method is the speed, ease of sample preparation & testing, relatively low cost, large numbers of indentation can be made quickly and the small volume of material required. Principally, it is the same as the microhardness measurement whereby the Vickers diamond indenter is driven into the specimen surface by a known load. When the indenter is removed, a characteristic pattern should be visible, comprising a central indentation with radial cracks emanating from the corners as shown in Figure 3.1. The crack systems formed by the Vickers indenter are namely the Median or half-penny and the Palmqvist crack system (Lach et al., 2007; Kruzic et al., 2009; Behnamghader et al., 2011). For low toughness material such as HA, the crack system has been identified as the media type. Thus, the fracture toughness (K_{IC}) is determined from the equation 3.5 derived by Niihara (1985).

$$K_{Ic} = 0.203\left(\frac{c}{a}\right)^{-\frac{3}{2}}(H_v)(a)^{\frac{1}{2}} \qquad \text{(Eqn. 3.5)}$$

Where,

K_{Ic} = Fracture toughness

H_v = Vickers hardness

c = Characteristics crack length (i.e. L + a)

L = Average crack length (i.e. $L = \frac{L_1 + L_2 + L_3 + L_4}{4}$)

a = Half diagonal length of the indent

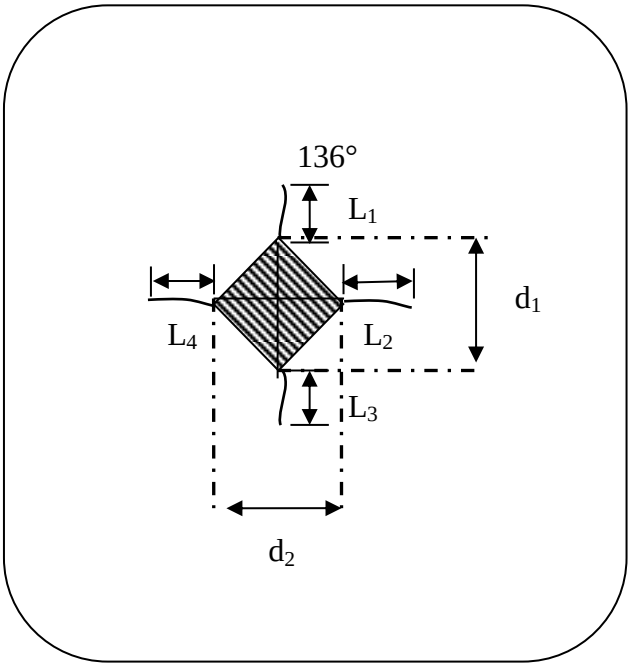

Figure 3.1: Schematic diagram of indentation on forsterite compact

3.6.4 Young's Modulus Evaluation

The Young's modulus of sintered samples is a measurement of the material's stiffness and resistance to elastic deformation (Callister Jr., 2007). It is defined as the ratio of stress over strain along that axis in the range of stress in which Hooke's law holds (McNaught et al., 1997). In this work, the Young's modulus by sonic resonance technique was determined for rectangular samples using a commercial testing instrument (GrindoSonic: MK5 "Industrial", Belgium). The instrument permits determination of the resonant frequency of a sample by monitoring and evaluating the vibrational harmonics of the sample by a transducer. The vibrations are physically induced in the sample by tapping. The modulus of elasticity was calculated using the experimentally determined resonant frequencies, according to standard test method ASTM E1876-09 (ASTM, 2009). The modulus of elasticity was calculated based on Equations 3.6 and 3.7.

$$E = 0.9465\left(\frac{mF^2}{w}\right)\left(\frac{L}{t}\right)^3 T \qquad \text{(Eqn 3.6)}$$

$$T = 1 + 6.585\left(1 + 0.0752\mu^2\right)\left(\frac{t}{L}\right)^2 - 0.868\left(\frac{t}{L}\right)^4 - \frac{8.34\left(1 + 0.2023\mu + 2.173\mu^2\right)\left(\frac{t}{L}\right)^4}{1 + 6.338\left(1 + 0.1408\mu + 1.53\mu^2\right)\left(\frac{t}{L}\right)^2}$$

(Eqn. 3.7)

E = Young's modulus

m = Mass of bar

F = Fundamental resonant frequency of bar in flexural (Hz)

w = width of bar

L = Length of bar

t = Thickness of bar

T = Correction factor for fundamental flexural mode to account for finite thickness of Bar

μ = Poisson ratio, taken as 0.28 (Grenoble et al., 1972)

3.6.5 Phase Stability

X-Ray diffraction (XRD) provides information related to the crystal lattice of the material and characterize the crystalline phases present. It can also provide information pertaining to the degree of crystallization and the orientation texture in the material (Cullity & Stock, 2001). In the present research, phase analysis of synthesized forsterite powders were investigated using a X-Ray diffractometer (Geiger-Flex, Rigaku, Japan), at room temperature with Cu-Kα (λ=1.54 Å) as the radiation source using a scan speed and step scan of 0.5°/min and 0.02° respectively, at 25 kV and 15 mA.

The average crystallite size (L) of forsterite nanopowder was calculated from the peak broadening in a XRD diffraction pattern associated with a particular planar reflection from within the crystal unit cell using Scherrer's formula (equation 3.8), (Cullity & Stock, 2001). Three most prominent diffraction peaks at 2θ (35.86°, 36.662°, 52.418°) were selected for the measurement and the average value was taken.

$$L = \frac{0.9\lambda}{\beta \cos\theta} \qquad \text{(Eqn 3.8)}$$

Where,

L = Crystallite size (m)

λ = Wavelength (0.154056 nm)

β = Peak width, FWHM, °

θ = Bragg angle, °

In this study, crystallite size was calculated from prominent forsterite peaks at 2θ =35°, 36° and 52°. X-ray diffraction was used to test if there were any significant changes to the phases of forsterite samples after sintering and to provide information related to the crystal lattice of the material. Thereafter, the peaks were then compared to standard reference JCPDS-ICCD (Joint Committee of Powder Diffraction Standard – International Centre for Diffraction Data) files for forsterite as shown in Table 3.1. The details of the said JCPDS-ICCD reference files are attached in the Appendix B.

Table 3.1: The 5 referred JCPDS phases

Phase	Chemical Equation	JCPDS PDF No.
Forsterite	Mg_2SiO_4	34-0189
Magnesium Oxide	MgO	43-1022
Talc	$Mg_3SiO_4O_{10}(OH)_2$	13-0558
Proto-enstatite	$MgSiO_3$	11-0273
Clino-enstatite	$MgSiO_3$	19-0769

3.6.6 Microstructure Observation

The Zeiss AURIGA FESEM (Field emission scanning electroscope) was used to observe the microstructure features of the synthesized forsterite powder and sintered compacts. The sintered forsterite compacts were thermal etched to delineate the grain boundaries to produce better images. The thermal etch temperature is 50°C below the sintering temperature using a ramp rate of 10°C/min and holding time of 30 minutes. After thermal etching, the forsterite compacts were secured on the FESEM metal mount with double sided carbon tape.

3.6.7 Quenching Experiment

An additional four green samples were sintered using conventional sintering method with temperature profile of 1000°C, 1200°C, 1400°C, 1500°C and ramp rate of 10°C/min. The sintered forsterite compacts were immediately removed from the furnace upon reaching the respective sintering temperatures and dropped into ice cold water. All the four forsterite compacts cracked naturally during the quenching process and the samples were dried in an oven (Memmert, Germany) at 70°C for 4 hours. The quenched samples were subjected to FESEM analysis.

3.6.8 Grain Size Measurement

FESEM micrographs of sintered forsterite were used to determine the grain size by using the line intercept method following ASTM E112-13 standards (ASTM, 2013). A straight line known as test line is drawn from the diagonal of the micrograph from one corner to the opposite corner. The above step was repeated for a similar test line drawn on the opposite diagonal. The average grain size was calculated based on the following Equation 3.9 and 3.10 (Mendelson, 1969).

$$\bar{D} = 1.56\,\bar{L} \qquad \text{(Eqn. 3.9)}$$

Where,

$\bar{D}$ = Average grain size

$\bar{L}$ = Average interception length

$$\bar{L} = \frac{C}{MN} \qquad \text{(Eqn 3.10)}$$

Where,

C = Total length of test line

M = Magnification of FESEM micrograph

N = Number of intercepts

The calculation of number of intercepts (N) consists of 3 types of scores. The first type is when the end points of test line is touching a grain boundary which is given a score of '0.5' at each end point. The second type is a tangential intersection with grain boundary which is given a score of '1'. The third type is when there is intersection with three or more grains which is given a score of '1.5'. The definition for number of intercepts is illustrated in Figure 3.2.

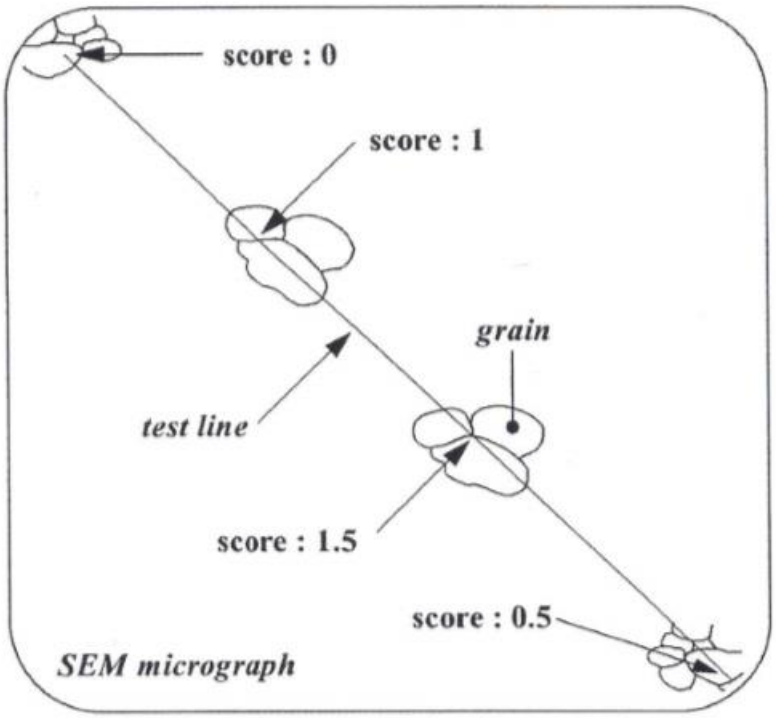

Figure 3.2: Definition for scores based on number of intersections (Ramesh, 1997)